ChemComm

Accepted Manuscript

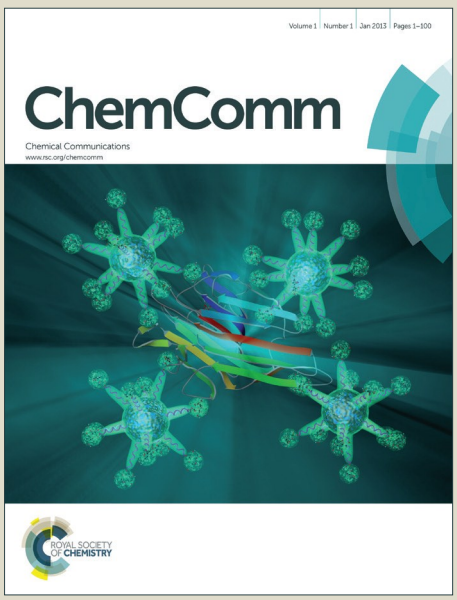

ROYAL SOCIETY OF CHEMISTRY

www.rsc.org/chemcomm

ChemComm

COMMUNICATION

Monitoring structural changes in intrinsically disordered proteins with QCM-D: Application to the bacterial cell division protein ZipA

Received 00th January 20xx,
Accepted 00th January 20xx

DOI: 10.1039/x0xx00000x

www.rsc.org/

Pablo Mateos-Gil,[a,b] Achilleas Tsortos,[c,*] Marisela Velez[a] and Electra Gizeli[c,d,*]

The QCM-D's sensitivity to molecular hydrodynamic properties is applied in this work to study conformational changes of the intrinsically disordered protein ZipA. Acoustic measurements can clearly follow ZipA's unstructured domain expansion and contraction with salt content and be correlated to changes in the hydrodynamic radius of 1.8 nm or less.

Intrinsically disordered proteins (IDPs) contain long regions without a well defined three dimensional structure. Despite the lack of structure, recent accumulation of evidence has shown that IDPs are involved in several cell processes in vivo[1, 2] and suggest an association with disease such as cancer and neurodegenerative disorders[3]. An area of particular interest is their regulatory role near membrane surfaces[4]. Disorder in protein domains defies the central dogma of structural biology, i.e., that protein function is given by its 3-D folded structure, pointing out the singularity of IDPs as the disorder-to-function relationship. Therefore, structural characterization of disorder, i.e., measuring the size and shape of the unstructured region, is crucial to better understanding how proteins of this new class carry out specific molecular tasks. However, a main constrain to study IDPs is the difficulty of applying X-ray crystallography, because of lack of crystals, and NMR[5] or FRET[6, 7] due to the necessity of sophisticated and expensive labeling. As alternatives, X-ray[8], neutron[9] and light scattering sometimes combined with intrinsic viscosity measurements[10] can be employed to this end.

Quartz crystal microbalance with dissipation monitoring (QCM-D) is an acoustic wave sensor for studying interfacial adsorption phenomena. This label-free technique has been extensively applied to quantify the density and mechanical properties of biomolecular layers formed onto the sensor surface; changes in the frequency of the wave (Δf) and energy dissipation (ΔD) obtained upon molecular binding have been used in combination with Voigt-type models to derive the thickness and mass content of the equivalent bio-film[11, 12]. Two-dimensional simulations employing the finite element method (FEM)[12, 13] and other methods[14] have also been useful in analyzing the hydrodynamic interactions at the sensor surface obtaining descriptions of the immobilized particles. Moreover, the QCM-D has been used to determine the size of a 30 nm mosaic virus[15], adsorbed nm-size liposomes[13, 15] and metallic and polymer nanoparticles[16] deposited on surfaces. An alternative approach presented recently relates the acoustic ratio (ΔD/Δf, i.e., energy dissipation per unit mass) to the hydrodynamic size and shape of surface-bound biomolecules considering them as discrete objects[17, 18]; in addition, it was shown that the acoustic ratio can be directly related to the intrinsic viscosity [η] of the attached biomolecules, where [η] is a direct measure of molecular conformation (i.e., shape and size). This methodology has opened the gate for new QCM-D based structural studies. Remarkably, it has been successful in quantifying the length, curvature and helical structure of single, double or triple stranded DNA[19-21]; it has also been used to characterize in real time conformational transitions such as DNA nanoswitching triggered by ions in the buffer[22] and hybridization[19, 20]. To date there has been a limited number of reports[23, 24] regarding IDP conformation studies using acoustic biosensors. Here we extend the discrete-molecule approach to the real time study of IDPs reversible expansion and collapse.

As a model system we studied the conformation of ZipA a membrane-anchored protein belonging to the bacterial cell division machinery of E. coli, containing a long disordered region enriched in both prolines and glutamines (P/Q) plus charged aminoacids, a distinctive feature of IDPs[3]. This unstructured region, between the short N-terminal transmembrane helix (aa 1-25) and the C-terminal globular domain of ZipA (aa 189-328)[5, 25], is a flexible linker able to undergo conformational transitions[26]. Electron microscopy and FRET studies showed that the disordered domain may stretch over a length from 8 to 20 nm in solution[7, 26]. Interface studies performed with ellipsometry revealed that ZipA layers increase in

[a] Instituto de Catálisis y Petroleoquímica (ICP-CSIC), c/MarieCurie 2, Cantoblanco, 28049 Madrid, Spain
[b] current address Department of Biotechnology & Biophysics, University Wuerzburg, Germany
[c] Institute of Molecular Biology & Biotechnology, FO.R.T.H, Vassilika Vouton, 70013, Heraklion, Greece
[d] Department of Biology, University of Crete, Vassilika Vouton, 71110, Heraklion,
* Corresponding authors: gizeli@imbb.forth.gr; tsortos@imbb.forth.gr
Electronic Supplementary Information available: see DOI: 10.1039/x0xx00000x

thickness from 10 to 20 nm under lateral compression[27], and atomic force microscopy suggested a different degree of stretching of the ZipA unstructured domain induced by the lipid head charges when ZipA is anchored and oriented onto supported lipid bilayers (SLBs)[28]. The fact that protein stretching is surface-charge dependent suggests that solution salt concentration can modulate the compactness of this non-structured charged domain.

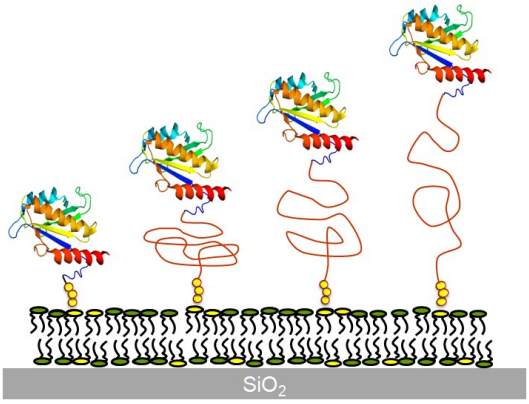

Fig. 1 Scheme illustrating the architecture of His-tagged constructs of ZipA bound to a lipid bilayer containing PC (90%) and NTA (10%) chelating lipids (yellow heads). *Left*: s2ZipA comprising only the N-terminal His-tag anchor (yellow beads) and the globular domain. *Right*: s1ZipA comprising the anchor plus the unstructured domain plus the globular domain, shown at three different expansions of the coiled part.

In this work, we used a well-tested platform, a supported lipid bilayer[29] (SLB), for anchoring two His-tagged soluble constructs of ZipA that lack the transmembrane helical domain. The first construct, s1ZipA, comprises both the globular (140 aa) and disordered (162 aa) parts while the second, s2ZipA, only the globular one; both contain a 21 aa-long His_6 peptide at the N-terminus that serves to anchor the proteins to the SLB through the standard PC/NTA-Ni-His reaction scheme (Fig. 1).

In a typical experiment, we first monitored the formation of the SLB onto the silica surface of the QCM-D sensor (Fig. S1). Final frequency and dissipation shifts, recorded at 35MHz and upon injection of the liposome solution, were $\Delta f \approx 200$ Hz (normalized change $\Delta f_7 = \Delta f/7 = 28$ Hz) and $\Delta D \approx 0.3 \times 10^{-6}$ respectively, verifying the formation of a homogeneous bilayer[30]. Subsequent addition of protein solutions led to surface attachment of s1ZipA and s2ZipA to the SLB containing 10% NTA lipids. The absence of binding to bilayers lacking NTA groups and the complete elution of surface bound proteins by 200 mM imidazole confirmed the specificity of the binding (Fig. S2). We identified appropriate concentration ranges (Fig. S3) to obtain stable signals which led to maximum frequency shifts of ≈ 210 and 100 Hz for s1ZipA and s2ZipA, respectively.

To study structural changes of the disordered region of ZipA, we monitored in real time the frequency and energy dissipation shifts induced by s1ZipA and s2ZipA during the exchange of protein adsorption buffer (TMK500) with buffers of decreasing salt content (TK500/50/5/0) (Fig. 2). The larger signals obtained during the addition of s1ZipA were attributed to the presence of the unstructured domain in the s1 construct as opposed to the s2 one. Furthermore, Fig. 2 shows that the subsequent reduction of buffer salt content only affected the acoustic signal of s1ZipA. To unambiguously attribute this response to conformational changes in the unstructured domain of ZipA, we subtracted ΔD and Δf obtained when buffers were passed over bare SLBs (Fig. S4).

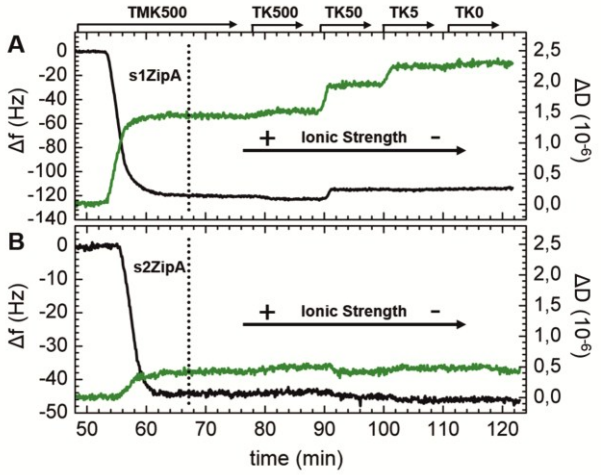

Fig. 2 Frequency (black) and energy dissipation (green) signals obtained upon addition of His-tagged soluble constructs of (A) s1ZipA and (B) s2ZipA followed by rinse with buffers of decreasing salt content (TMK500 and TK500/50/5/0 correspond to buffers with 500, 50, etc. mM KCl, see Table S1); buffer exchanges are indicated by horizontal arrows.

Experiments carried out with different protein concentrations were used to calculate the acoustic ratio ΔD/Δf of each construct as a function of surface coverage, in each of the five buffers. Figure 3 shows that the absolute acoustic ratio values as well as their dependency on surface coverage (indicated by the mass-sensitive frequency signal) differ substantially for the two proteins. Specifically, s1ZipA gives higher acoustic ratios which are affected more by the buffer salt content and less by surface coverage; the opposite behavior is observed with s2ZipA. For comparing the ratios of the two proteins in the same buffer, we calculated the extrapolated acoustic ratios at zero surface coverage, theoretically corresponding to the binding of one molecule.

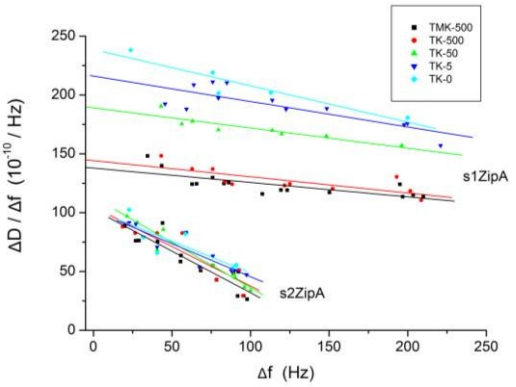

Fig. 3. The dependence of the acoustic ratio on surface coverage during the binding of s1 and s2ZipA, as a function of the salt concentration. Each point corresponds to a single experiment taken at equilibrium. The max values of 100 and 210 Hz correspond to stable monolayer coverage for s1 and s2ZipA, respectively.

These values are plotted versus the salt content of the running buffer in Fig. 4 (blue lines). In the case of s1ZipA a clear transition in ΔD/Δf (from 138±8 to 239±16 x 10^{-10}/Hz) is observed when salt content is depleted whereas the ratio remains constant (105±8 x 10^{-10}/Hz) at all ionic strengths for s2ZipA. Importantly, the acoustic ratio of s1ZipA protein responds to this increase/decrease of ionic strength in a perfectly reversible manner (see Fig. S5).

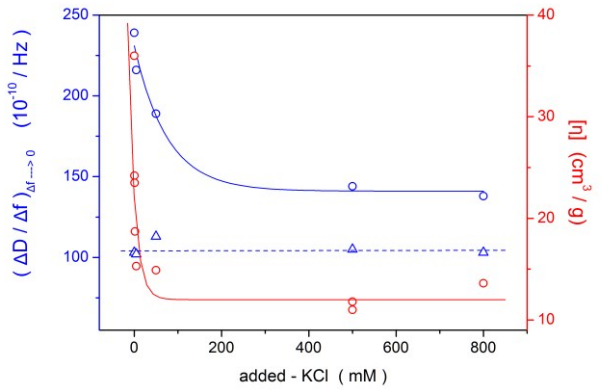

Fig. 4. The dependence of the acoustic ratio (intercepts from Fig. 3) at 35 MHz (blue) and intrinsic viscosity of s1ZipA (red), on the added salt concentration, at 25 °C. Dashed line refers to s2ZipA, solid lines correspond to s1ZipA.

The discrete-molecule binding theory[17, 18] suggests that the acoustic ratio is proportional to the intrinsic viscosity [η] of any biomolecule, where [η] is a measure of the molecular hydrated volume[31] expressed in cm^3/g. This has been proven true for DNAs of various lengths and for a great variety of shapes[19-22], but has never been shown for proteins. In order to confirm this we performed independent measurements of the intrinsic viscosity of s1ZipA by viscometry (see SI). Figure 4 (red) shows the results plotted against the buffer salt content. As can be seen, the dependence of [η] on the concentration of the KCL salt is similar to the one obtained for ΔD/Δf measurements; they both decay fast with increasing salt content (blue and red solid curves).

The almost two-fold decrease in the acoustic ratio of s1ZipA as the buffer salt is increased can be interpreted as the contraction of the protein molecule. Since the same treatment does not affect the acoustic ratio of s2ZipA, one can safely conclude that the part of the protein molecule responsible for this effect is its unstructured domain. The dependence of [η] on the ionic strength of the solution in the case of polyelectrolytes[32, 33] is in agreement with the data shown in Fig.4. Proteins are considered to behave as weak polyelectrolytes bearing both positive and negative charges, exhibiting sometimes sensitivity on *pH* and/or ionic strength. This behavior can result in structural rearrangements reflected in changes in hydrodynamic quantities such as the radius of gyration R_g, radius of hydration R_h, chain end-to-end distance R_{ee} or intrinsic viscosity [η][32-36]. Similarly, molecules end-tethered at surfaces also display a swelling/expanding behavior, just like in bulk solution, when salt reduces[24, 37, 38]. In the case of s2ZipA, the well-folded globular part does not respond with significant size changes to ionic strength variation, as expected for compact, densely packed globular molecules[39, 40]. In contrast, the unstructured part with its open coil-like shape and the presence of charged groups in its sequence is more prone to change and is apparently responsible for the observed changes in [η]. These results provide further experimental evidence in support of the previously suggested hydrodynamic basis of acoustic biosensing[17, 18, 22].

The good correlation between [η], measured in bulk solution and acoustic ratio, measured with the protein oriented at a surface, points to bulk size preservation upon immobilization, indicating minimal interaction with the surface and among the protein chains[27, 41]. Apparently, this is the case for both the globular domain and the whole ZipA molecule on the lipid bilayer-covered sensor surface where non-specific binding was not experimentally observed. Nevertheless, the observed dependency of the acoustic ratio on surface coverage indicates a certain degree of lateral protein-protein interaction, an effect which is more pronounced in the case of s2ZipA (Fig. 3). Then, the proposed methodology of obtaining the extrapolated ratio at zero coverage $(\Delta D/\Delta f)_{\Delta f \to 0}$, is the way to ensure that the acoustic ratio used, indeed, refers to surface-attached molecules that exhibit zero lateral cross-talk.

In order to confirm that the changes in acoustic ratio observed can be associated to the compaction of the protein, we calculated R_h from the intrinsic viscosity data on s1ZipA under variable salt content (See SI and Fig. S6). We found that R_h reduces from ≈ 5.9 nm at the protein's most expanded state, to ≈ 4.1±0.1 nm at its most contracted. The reliability of this estimate was checked against an independent method using the HYDROPRO bead model simulation software (see SI); this method[42] gives an R_h = 4.0 nm which is practically identical to our value. The surface attached protein is expected to undergo the same conformation changes under the same conditions, so we conclude that the changes of ΔD/Δf as a function of salt concentration reflect this compaction. This direct correlation of ΔD/Δf to bulk hydrodynamic quantities, the intrinsic viscosity in this case, indicates that acoustic sensing can be indeed used to monitor real-time conformational changes on proteins at an interface.

Finally, we used the classic Sauerbrey equation in order to derive from acoustic data an estimate of the orientation of single s1ZipA molecules at the surface. From simple geometry calculations and the molecular weight one obtains

$$S(nm^2/molecule) = \frac{Mw}{15.2 * \Delta F_{35}^{monolayer}} \qquad \text{Eq. 1}$$

From Eq. 1 and Fig. 3 ($\Delta F_{monolayer}$ ≈ 210 and 100 Hz for the s1 and s2ZipA, respectively), we estimate that for close-packed monolayer coverage the projection geometrical radius R_{xy} for both proteins is equal to ≈ 1.9 nm. Since this is the size of the globular part[5, 25] one may infer that the coil part in s1ZipA is mostly extended vertically (along the z-axis) from the surface as if in a brush formation (as shown in Fig.1), in accordance to recent findings[27].

This is the first time that the size-dependent hydrodynamic parameters [η] and R_h are directly linked to acoustic measurements of surface anchored IDPs. The intrinsic viscosity is capable of discriminating molecular size changes of ≈ 1.8 nm or less, and here we confirm that acoustic measurements can achieve equal sensitivity, validating their use to study conformational changes of

IDPs at the interface. In applying the methodology in general we note the following: a) the approach described here cannot be applied in the case of direct physisorption; care must be taken that there is zero non-specific binding and this requires searching for an appropriate substrate, b) the molecule must be immobilized without significantly distorting its conformation and c) to obtain correct acoustic ratios it is important to check for the existence of lateral cross-talk among the molecules at the interface; if these are present, the use of the $(\Delta D/\Delta f)_{\Delta f \to 0}$ value is necessary.

AT and EG acknowledge the financial support of EC (FP7/ICT & Regpot Grants 317742 & 316223) and GSRT/Ministry of Education, Greece and European Regional Development Fund (Sector Operational Program: Competitiveness and Entrepreneurship, NSRF 2007-2013)/EC (KRIPIS-BIOSYS (MIS-448301). PMG, MV and EG thank COST Action TD1003. We also thank V. Tseliou for technical assistance and P. Lopez-Navajas for the protein mutants.

References

1. H. J. Dyson and P. E. Wright, *Nat. Rev. Mol. Cell Biol.*, 2005, **6**, 197-208.
2. P. E. Wright and H. J. Dyson, *Nat. Rev. Mol. Cell Biol.*, 2015, **16**, 18-29.
3. V. N. Uversky, *Protein Sci.*, 2013, **22**, 693-724.
4. D. J. Busch, J. R. Houser, C. C. Hayden, M. B. Sherman, E. M. Lafer and J. C. Stachowiak, *Nat. Commun.*, 2015, **6**, 7875.
5. F. J. Moy, E. Glasfeld, L. Mosyak and R. Powers, *Biochemistry*, 2000, **39**, 9146-9156.
6. E. Sherman and G. Haran, *Proc. Natl. Acad. Sci. USA*, 2006, **103**, 11539-11543.
7. T. Ohashi, S. D. Galiacy, G. Briscoe and H. P. Erickson, *Protein Sci.*, 2007, **16**, 1429-1438.
8. G. Damaschun, H. Damaschun, K. Gast and D. Zirwer, *J. Mol. Biol.*, 1999, **291**, 715-725.
9. H. K. Murnen, A. M. Rosales, A. V. Dobrynin, R. N. Zuckermann and R. A. Segalman, *Soft Matter*, 2013, **9**, 90-98.
10. R. B. Hawkins and A. Holtzer, *Macromolecules*, 1972, **5**, 294-&.
11. M. V. Voinova, M. Rodahl, M. Jonson and B. Kasemo, *Phys. Scripta*, 1999, **59**, 391-396.
12. I. Reviakine, D. Johannsmann and R. P. Richter, *Anal. Chem.*, 2011, **83**, 8838-8848.
13. E. Tellechea, D. Johannsmann, N. F. Steinmetz, R. P. Richter and I. Reviakine, *Langmuir*, 2009, **25**, 5177-5184.
14. J. S. Ellis and M. Thompson, *Chem. Sci.*, 2011, **2**, 237-255.
15. I. Reviakine, M. Gallego, D. Johannsmann and E. Tellechea, *J. Chem. Phys.*, 2012, **136**, 084702.
16. A. L. J. Olsson, I. R. Quevedo, D. Q. He, M. Basnet and N. Tufenkji, *ACS Nano*, 2013, **7**, 7833-7843.
17. A. Tsortos, G. Papadakis, K. Mitsakakis, K. A. Melzak and E. Gizeli, *Biophys. J.*, 2008, **94**, 2706-2715.
18. A. Tsortos, G. Papadakis and E. Gizeli, *Biosens. Bioelectron.*, 2008, **24**, 836-841.
19. A. Tsortos, A. Grammoustianou, R. Lymbouridou, G. Papadakis and E. Gizeli, *Chem. Commun.*, 2015, **51**, 11504-11507.
20. G. Papadakis, A. Tsortos, F. Bender, E. E. Ferapontova and E. Gizeli, *Anal. Chem.*, 2012, **84**, 1854-1861.
21. G. Papadakis, A. Tsortos and E. Gizeli, *Biosens. Bioelectron.*, 2009, **25**, 702-707.
22. G. Papadakis, A. Tsortos and E. Gizeli, *Nano Lett.*, 2010, **10**, 5093-5097.
23. O. Shur, J. Wu, D. M. Cropek and S. Banta, *Protein Sci.*, 2011, **20**, 925-930.
24. N. Srinivasan, M. Bhagawati, B. Ananthanarayanan and S. Kumar, *Nat. Commun.*, 2014, **5**, 5145.
25. L. Mosyak, Y. Zhang, E. Glasfeld, S. Haney, M. Stahl, J. Seehra and W. S. Somers, *Embo J.*, 2000, **19**, 3179-3191.
26. T. Ohashi, C. A. Hale, P. A. J. de Boer and H. P. Erickson, *J. Bacteriol.*, 2002, **184**, 4313-4315.
27. I. Lopez-Montero, P. Lopez-Navajas, J. Mingorance, G. Rivas, M. Velez, M. Vicente and F. Monroy, *Faseb J.*, 2013, **27**, 3363-3375.
28. P. Mateos-Gil, I. Marquez, P. Lopez-Navajas, M. Jimenez, M. Vicente, J. Mingorance, G. Rivas and M. Velez, *Biochim. Biophys. Acta - Biomembr.*, 2012, **1818**, 806-813.
29. R. P. Richter, K. K. Hock, J. Burkhartsmeyer, H. Boehm, P. Bingen, G. L. Wang, N. F. Steinmetz, D. J. Evans and J. P. Spatz, *J. Am. Chem. Soc.*, 2007, **129**, 5306-5307.
30. N. J. Cho, C. W. Frank, B. Kasemo and F. Hook, *Nat. Protoc.*, 2010, **5**, 1096-1106.
31. S. E. Harding, *Prog. Biophys. Mol. Biol.*, 1997, **68**, 207-262.
32. C. E. Brunchi, S. Morariu and M. Bercea, *Colloid Surf. B-Biointerfaces*, 2014, **122**, 512-519.
33. O. Smidsrod and A. Haug, *Biopolymers*, 1971, **10**, 1213-&.
34. Y. Kantor and M. Kardar, *Europhys. Lett.*, 1994, **27**, 643-648.
35. A. Tsortos, G. Papadakis and E. Gizeli, *Biopolymers*, 2011, **95**, 824-832.
36. J. G. Hernandez Cifre and J. Garcia de la Torre, *Polym. Bull.*, 2014, **71**, 2269-2285.
37. J. Feng, K. Y. Wong, G. C. Lynch, X. L. Gao and B. M. Pettitt, *J. Phys. Chem. B*, 2009, **113**, 9472-9478.
38. E. B. Zhulina and M. Rubinstein, *Soft Matter*, 2012, **8**, 9376-9383.
39. C. Tanford and J. C. Buzzell, *J. Phys. Chem.*, 1956, **60**, 225-231.
40. J. C. Buzzel and C. Tanford, *J. Phys. Chem.*, 1956, **60**, 1204-1207.
41. M. Kawaguchi, K. Hayashi and A. Takahashi, *Macromolecules*, 1984, **17**, 2066-2070.
42. D. Amoros, A. Ortega and J. Garcia de la Torre, *J. Chem. Theory Comput.*, 2013, **9**, 1678-1685.